2008 Water Reactor Fuel Performance Meeting
October 19~23, 2008, Renaissance Seoul Hotel, Seoul, Korea
www.wrfpm2008.org
Paper No. 8126

The Influence of Hydrogen on the Deformation Behavior of Zircaloy-4

M. E. Flanagan [1,3], D. A. Koss [2], and A. T. Motta [1]
[1] *Department of Mechanical and Nuclear Engineering, The Pennsylvania State University, University Park, PA 16802*
[2] *Department of Materials Science and Engineering, The Pennsylvania State University, University Park, PA 16802*
[3] *U. S. Nuclear Regulatory Commission, Rockville, MD 20852*
Tel: +1 301 415 3965 , Fax:+1 301 415 5062 , Email:michelle.flanagan@nrc.gov

Abstract – *The deformation behavior of Zr-based cladding forms a basis for fuel behavior codes and affects failure criteria; as such, it is critical to reactor safety. The present study examines the influence of hydrogen on the uniaxial deformation behavior of hydrided cold worked and stress-relieved Zircaloy-4 plate material. Specimens of various orientations (i.e., stress axis aligned with the rolling direction, the transverse direction, or normal-to-the plate surface direction) were tested in compression at a range of temperatures (25°, 300°, and 400°C), and strain rates (from 10^{-4}/s to 10^{-1}/s). Contrasting the deformation behavior of the material containing ~45 wt ppm H with that of the material containing ~420 wt. ppm H shows that increasing H content (a) causes a small decrease in the 0.2% yield stress that is eliminated at 1.0% flow stress, (b) increases the strain hardening in the rolling direction but not in the other orientations, (c) has no effect on the temperature dependence of the strain hardening, and (d) does not affect the strain-rate hardening behavior. Increasing H content also has no observable effect on the high degree of plastic anisotropy of this plate material which is manifested in difficult through-thickness deformation, resulting in high flow stresses for specimens oriented in the normal-to-plate-surface direction.*

I. INTRODUCTION

The influence of temperature on the deformation behavior of zirconium alloys (and Zircaloy-4 cladding in particular) has been the subject of several investigations; see for example [1-5]. As a result, the yield stress, strain hardening, and strain-rate hardening responses of these alloys have been fairly well established and serve as a basis for current computational codes. Similarly, numerous studies have identified the strong influence of hydrogen and hydrides on the fracture behavior of zirconium-based alloys in general and Zircaloy cladding in particular [2-12]. In contrast, relatively little is known of the effect of hydrogen *on the deformation behavior* over a range of temperatures of these plastically anisotropic alloys. The purpose of this investigation is to examine the uniaxial deformation behavior of Zircaloy-4 as a function of hydrogen level (~45 to ~420 wt ppm), temperature (25°, 300°, and 400°C), and strain rate (10^{-4}/s to 10^{-1}/s). Strongly textured plate is used as a model material to allow tests to be performed as a function of orientation of deformation axis (rolling direction, transverse direction, and normal-to-plate surface direction) and to obtain data on the influence of hydrogen content on the yield strength, strain hardening, and strain-rate hardening as well as plastic anisotropy of Zircaloy-4. Such data should serve as a basis for developing more robust and accurate temperature-dependent constitutive relationships to be developed for cladding tube materials.

II. EXPERIMENTAL PROCEDURE

The material used in this study was 4.5 mm thick Zircaloy-4 plate obtained from Teledyne Wah-Chang. The material was hot rolled, and then 30% cold rolled and stress relief annealed at 500°C for one hour in a vacuum furnace at 10^{-6} Torr. This processing procedure resulted in a microstructure consisting of slightly elongated grains measuring about 15 microns in the rolling direction and about 10 microns in the normal direction. Metallography shows no change in grain size and grain shape after stress relief, indicating no recrystallization has taken place. The chemical composition was measured and found to be Zr-1.52Sn-0.23Fe-0.136O-0.11Cr-0.020C-0.0045H wt. %. The texture of the plate was measured using X-Ray Diffraction to plot a basal pole figure and to calculate Kearns factors for the plate material. The calculated basal pole figure for the plate material is shown in Fig. 1.

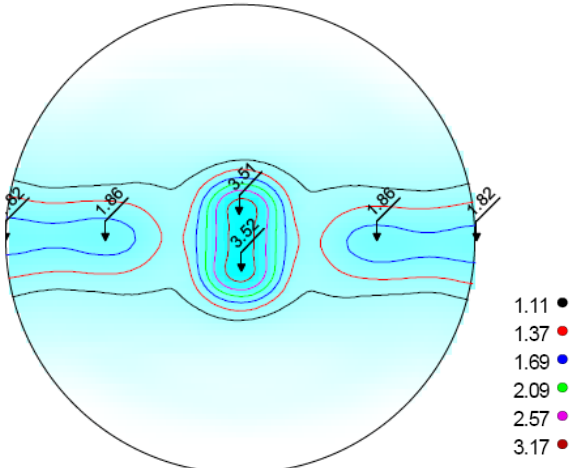

Figure 1. Basal pole figure of Zircaloy-4 plate material.

The Kearns factors were measured to be $f_N = 0.49$, $f_R = 0.188$ and $f_T = 0.322$. Typical cladding Kearns factors are $f_N = 0.66$, $f_R = 0.06$ and $f_T = 0.28$ [1].

Hydrogen was introduced into the material by gas-charging using the following procedure. To facilitate the absorption of hydrogen, the protective oxide was removed by chemical etching using a mixture of 1 part hydrofluoric acid, 10 parts nitric acid, 10 parts H_2O. Within 15 minutes, the specimen was inserted into an ultra high vacuum system and subsequently a thin layer of nickel was vapor deposited onto the sample to protect the surface and allow hydrogen uptake. The Zircaloy was then gas-charged by cycling the specimens in a 12.5% hydrogen-87.5% argon gas mixture at 450°C for 1 hr followed by cooling to 200°C for an additional 0.5 hr in vacuum. The total charging process involved 3-5 cycles, and the specimens were slowly cooled to room temperature after the last cycle. The cyclic hydrogen charging procedure resulted in the formation of a uniform distribution of hydrides throughout the thickness of the plate, as shown in Fig. 2.

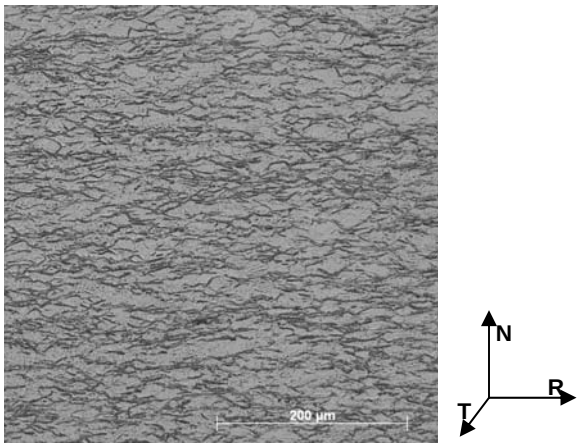

Figure 2. Light microscope micrograph of hydrided material, 420 wt. ppm +/- 50 ppm.

As in cold worked stress relieved Zircaloy cladding, the hydrides are elongated and aligned parallel to the plate surface. A thin hydride rim occasionally formed at the surface, and in those cases, this layer was removed by mechanical polishing. The hydrogen content of each sample was measured by hot vacuum extraction analysis, which showed that the hydrogen content was 45 wt ppm in the unhydrided samples, and 280, 400, and 420 wt ppm after hydrogen charging.

To perform compression testing, 4.5mm cubic specimens were fabricated with a one-to-one height to width ratio [13]. Uniaxial compression testing of these cube specimens was performed in the three orientations: the stress axis was aligned along either the rolling (designated R), the transverse (designated T), or the normal-to-the-plate-surface direction (designated N). When correlated with cladding tube directions, these orientations correspond to the axial, circumferential and radial cladding directions, respectively, as shown in Fig. 3. Some tensile tests were also performed on specimens with a 4:1 gauge length to width gauge ratio, and these specimens also had gauge widths of 7.5 mm. The initial strain rate in all tests was 10^{-3}/s.

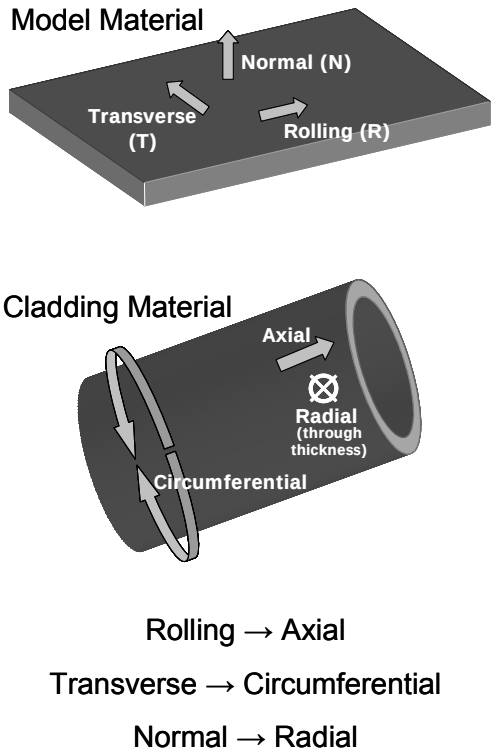

Figure 3. A schematic showing the nomenclature for test specimen orientation within the Zircaloy-4 plate examined in the present study and how it correlates to orientations within cladding tube.

In most postulated in-service and accident conditions such as in Pellet-Cladding Mechanical Interaction (PCMI) and over-pressurization, cladding loading is tensile [14]. Deformation behavior of metals is normally the same in tension and compression, provided that the testing procedure enables the material to deform uniformly along its length. To show that compression testing gives comparable results to tension in this case, Fig. 4 shows the stress-strain responses of unhydrided as well as unhydrided material in tension and compression. While the yield stress in tension is slightly lower, the strain-hardening behavior is identical for unhydrided material in tension and compression and for hydrided material in tension and compression, indicating similar deformation behavior in tension and compression. Although samples tested in compression were well lubricated in order to reduce friction during deformation, the small amount of friction experienced during compression testing that was not experienced during tensile testing could lead to the slightly higher compressive yield stress seen in this study. Therefore the deformation behavior observed in this study, performed in compression, should be relevant to in-service loading in tension. This is important because compression testing provides a means of avoiding tensile-induced necking instabilities at small strains so that accurate stress-strain responses at larger strains can be obtained.

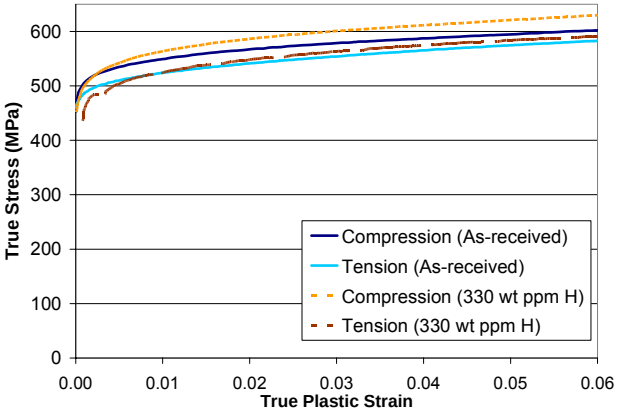

Figure 4. The stress-strain response of hydrided (300 wt ppm H) as well as unhydrided Zircaloy-4 plate as determined in tension and compression for specimens oriented along the long transverse direction of the plate; see Fig. 3.

III. RESULTS AND DISCUSSION

III.A. Yield Stress Behavior

Figure 5 shows the true stress-true strain behavior for (a) the rolling and (b) transverse directions, for unhydrided (solid lines) and hydrided (dashed lines), when tested at room temperature, 300ºC and 400ºC. A comparison of the yield stress values at the 0.2% offset strains in Fig. 5 shows similar values to yield stresses determined for cold-worked and stress-relieved Zircaloy cladding tubes at both room temperature and 400°C [15]. As shown in Fig. 5, the influence of hydrogen on the stress-strain response of the Zircaloy-4 depends on the orientation of the stress axis. When compressed along the rolling direction (Fig. 5a), the hydrided material yields at a lower stress with a more gradual transition from elastic to plastic behavior, especially in the vicinity of the proportional limit where the onset of plasticity is first detected. This behavior persists to elevated temperatures, but it is more pronounced at room temperature. As a result, the influence of hydrogen is to decrease both the proportional limit and the 0.2% yield stress for deformation along the rolling direction. In contrast, for specimens oriented along the long transverse orientation, Fig. 5b shows that the transition from elastic to plastic behavior is more abrupt, and in this orientation, the hydrides have only a minor effect in decreasing the 0.2% yield stress.

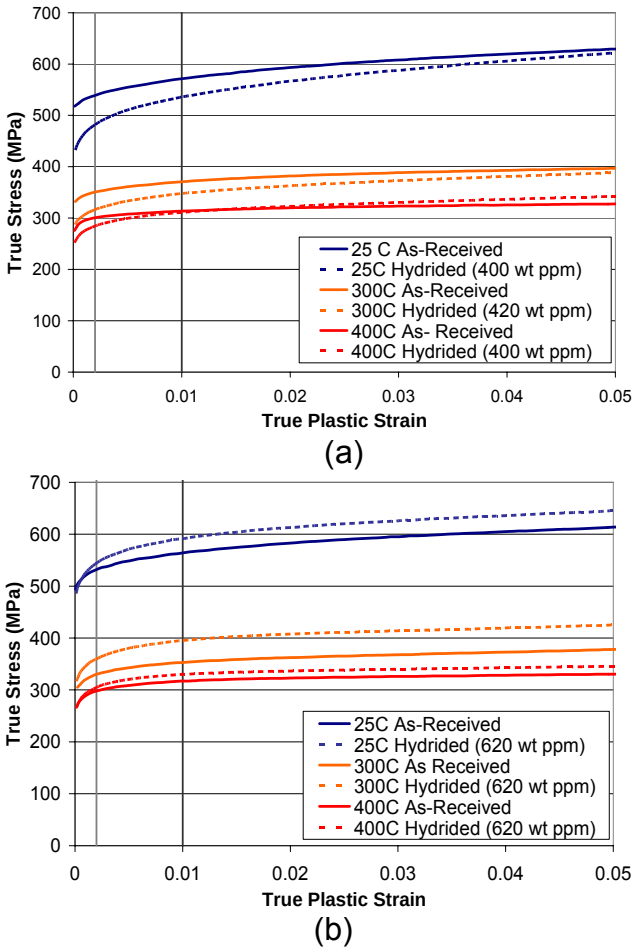

Figure 5. The stress-strain behavior of as-received and hydrided material in the (a) rolling and (b) transverse directions. The 0.02% and 1% yield limits are indicated.

The near-yield behavior and its sensitivity to hydrogen content and specimen orientation is shown more clearly in Fig. 6, where the normalized difference (YD) between the "yield" stress at 1.0% strain ($YS_{0.01}$) and that at the conventional 0.2% offset yield stress ($YS_{0.002}$) defined as

$$YD=(YS_{0.01}) - (YS_{0.002})]/(YS_{0.01})] \quad (1)$$

Defining YD in this manner means that the gradual transition from elastic to plastic behavior and concomitant decrease of the proportional limit seen in Fig. 5a at room temperature results in a large value of YD, as depicted in Fig. 6. Summarizing the elastic-plastic transition behavior, Fig. 6 shows that this "gradual" yielding behavior is most pronounced at high hydrogen contents in specimens whose major deformation axis is along the rolling direction. While the effect is smallest for specimens aligned along the transverse direction, it still increases somewhat with hydrogen content. At 300 and 400°C, the transition from elastic to plastic is somewhat more abrupt than at room temperature and as a result the normalized yield stress difference parameter shows only a smaller increase with hydrogen content.

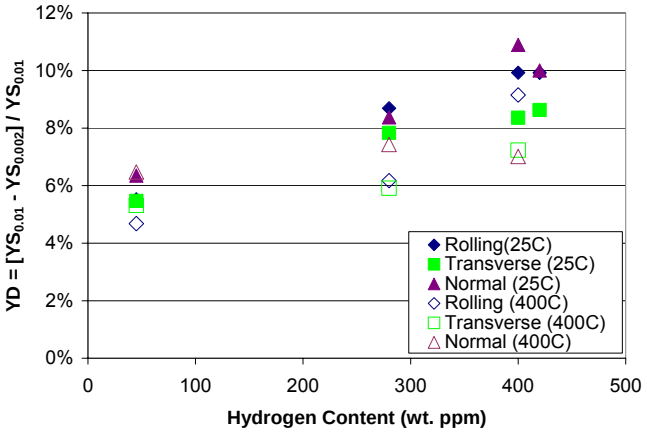

Figure 6. The normalized yield stress difference parameter as a function of hydrogen content.

The yielding behavior of metals has been understood for many years in terms of the classic dislocation dynamics concepts first proposed by Johnston and Gilman [16-18]. In this analysis, an abrupt yield point occurs when a very small initial mobile dislocation density multiples rapidly as the dislocations move with high velocities at the high stresses near yielding. Thus, abrupt yielding (or a yield drop as in steels) is a result of an "avalanche" of mobile dislocations that form very rapidly at the yield point. One consequence of this model is that if the metal is subject to a small pre-strain which acts to increase the initial mobile dislocation density, a more gradual yielding transition from elastic to fully plastic behavior will occur. In the present case of hydrided Zircaloy, it is also well known that due to the large differences in specific volume between zirconium hydrides and the zirconium alloy matrix, the formation of hydride precipitates is accommodated by a plastic zone of dislocations near the hydrides [19]. Thus we suggest that the behavior shown in Figures 5 and 6 result from the increased in the initial mobile dislocation resulting from the plastic zones associated with the hydrides. Given the crystallographic texture and alignment of the plate-like hydride precipitates (Fig. 2) and their plastic zones, the extent to which the plastic zones can contribute mobile dislocations will depend on the orientation of the stress axis. Thus, the yielding behavior would also likely be sensitive to the orientation of the stress axis, as observed.

As described above, the influence of hydrogen is to promote early yielding so that the 0.2% offset yield stress decreases somewhat with increasing hydrogen. However, this effect disappears if a 1% offset yield stress definition is employed. Fig. 7 shows the 1% offset yield stress as a function of hydrogen content. No significant effect of hydrogen is seen on the yield/flow stress at 1% plastic strain even though there is a small decrease of the 0.2% offset yield stress with increasing hydrogen content. This behavior is consistent for the three plate orientations studied. A previous study also observed no significant effect of hydrogen on the room temperature yield stress of hydrided Zircaloy-4 tubes [20].

II.B. Plastic Anisotropy Behavior

While the orientation of the stress axis has a small effect on the yield point transition of the Zircaloy-4, it has a significant effect on the magnitude of the yield stress. As also shown in Figure 7, specimens deformed along the axis oriented normal to the plate surface exhibit yield stresses nearly two times higher than those measured in either the rolling or transverse orientation. This effect clearly indicates the difficulty of activating through-thickness slip deformation, which is consistent with a strong basal texture such as shown in Fig. 1.

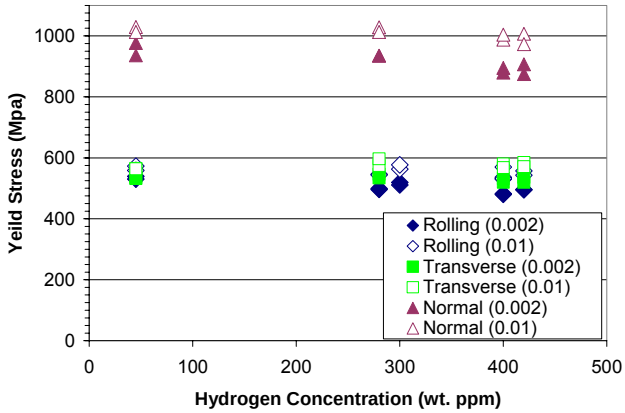

Figure 7. The yield stresses of Zircaloy-4 plate (as defined at either 0.2% or 1.0% offset strain) as a function of hydrogen for the three orientations of stress axes within the plate (Fig. 2).

The yielding behavior of materials with difficult through-thickness deformation is usually quantified in terms of Hill's quadratic yield criterion, which can be expressed in terms of the plastic anisotropy ratios R and P if the material exhibits planar isotropy, as does the present material [20]. If ε_R, ε_T and ε_N are the true plastic strains in the rolling, transverse and normal directions, respectively, then the parameters R and P are normally determined from tensile tests under conditions of uniform strain, such that R = ε_T /ε_N for a specimen loaded along the rolling direction and P = ε_R /ε_N for a tensile specimen loaded in the transverse direction. On the other hand, in the absence of tension-compression asymmetry (as demonstrated in Fig.4), the ratios (ε_T /ε_N) and (ε_R /ε_N) can also be obtained from compression testing by determining the accommodation of plastic strains in the two orientations transverse to the compression axis.

Table 1 shows the R and P values calculated from both room temperature tensile tests of unhydrided plate. In addition, the transverse strain path under through-thickness compression was determined from room temperature tests. The tensile test data show R ≅ 5.4 and P ≅ 4.2. It should be recalled that for plastically isotropic metals, R = P = 1.0. Thus, as also seen in Zircaloy cladding, the plate exhibits a strong degree of plastic anisotropy which is manifested in difficult through-thickness deformation and a high yield stress in the normal-to-the-plate-surface orientation.

Based on the Hill yield criterion and the values of R and P, it is possible to predict the ratio of the normal stresses required to induce yielding in equal-biaxial tension, which is a strain path of interest in reactivity-initiated accidents where cladding-pellet interactions can be significant.

TABLE I

Plastic strain ratios in orientations transverse to the deformation axis, averaged over all hydrogen contents in the case of compression results

Deformation in Rolling Dir. ε_T /ε_N (R-value)	Deformation in Transverse Dir. ε_R /ε_N (P-value)	Deformation in Normal Dir. ε_R /ε_T
5.4 (Tension)	4.2 (Tension)	0.7 (Compression)

If σ_{eq} is the Hill equivalent stress, then the ratio of the normal stresses required to yield the material in equal biaxial tension (σ_{EBT}) is given by the following relationship [21-22]:

$$\frac{\sigma_{EBT}}{\sigma_{eq}} = \left[\frac{P(1+R)}{P+R}\right]^{1/2} \quad (2)$$

In the present case, $\sigma_{eq} = \sigma_y$ (the uniaxial yield stress along either the rolling or transverse orientations) since the material exhibits planar isotropy. In addition, the Hill formulation indicates that the strain-path ($d\varepsilon_1/d\varepsilon_2$) associated with equal-biaxial tension is through-thickness compression of the plate with a strain-path of $d\varepsilon_1/d\varepsilon_2$ = P/R, where $d\varepsilon_1$ and $d\varepsilon_2$ are the respective minor strains in the plate transverse and rolling directions.

Relating the above analysis to the present study, we associate the *compressive* deformation behavior in the normal-to-plate-surface orientation to deformation behavior in equal-biaxial *tension* – recall that equal-biaxial tensile deformation in Fig. 3 must occur by through thickness deformation in the normal (N) direction. Thus, the compressive "equivalent" of equal biaxial tension should also be characterized by a strain path of $d\varepsilon_1/d\varepsilon_2$ = P/R. Given the P-values and R-values in Table 1, deformation in the plate normal orientation should thus be associated with a transverse strain ratio of $d\varepsilon_1/d\varepsilon_2$ = P/R ≈ 0.8. This predicted value is close to the experimentally observed value of 0.7 in Table 1 for compression in the plate normal orientation. As such, the strain-path behavior supports the equivalence of plastic deformation under a plate-normal compression mode to equal biaxial tension. In addition, using Eq. 2 and the R- and P-values at room temperature, we can also estimate the ratio of yield stresses in the normal orientation to that in either the rolling or transverse orientations. Those data indicate:

$$\frac{\sigma_{EBT}}{\sigma_{eq}} \cong \frac{\sigma_N}{(\sigma_y)_R} = \frac{\sigma_N}{(\sigma_y)_T} \cong 1.7 \text{ to } 1.8$$

for room for temperature behavior depending on whether compressive or tensile R and P values are used from Table 1. As shown in Fig. 8, this predicted estimate agrees well with the stress ratio experimentally observed at room temperature where $\sigma_N/\sigma_R \approx \sigma_N/\sigma_T \cong 1.8$. Thus, these results also support the equivalence of through-thickness compression to equal biaxial tension. Significantly, this ratio is roughly independent of either temperature or hydrogen content, implying that the plastic anisotropy is preserved to at least 400°C (also observed in Zircaloy-4 cladding tube by Delobelle et al, ref. 5), and it is not affected by the presence of hydrides.

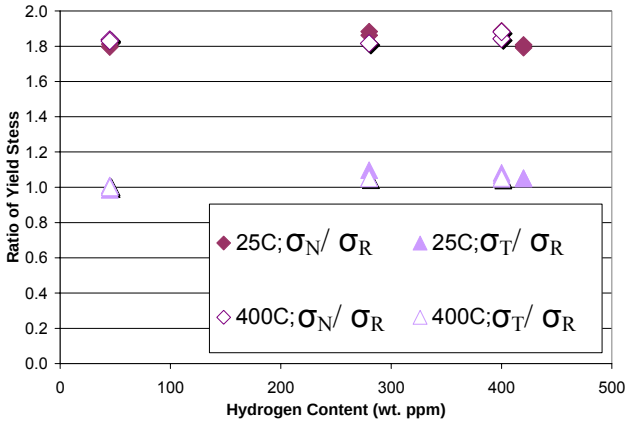

Figure 8 – The effect of hydrogen on yield stress anisotropy as defined by the ratio of the yield stress in the rolling orientation to that in either the normal-to-plate-surface or transverse orientations.

III.C. Strain Hardening Behavior

The material was assumed to obey the power-law stress-strain relationship given by

$$\sigma = k(\varepsilon_p)^n \qquad (3)$$

where k is the strength coefficient, n is the strain-hardening exponent and σ and ε_p are the true stress and true plastic strain, respectively. Thus the influence of hydrogen on strain hardening was examined by determining the strain-hardening exponent within the plastic strain range $0.01 \leq \varepsilon_p \leq 0.05$ during compression testing. It was found that during this strain range the specimen deformation was uniform, and the correlation coefficient of the n-value as determined from linear regression analysis of $\log\sigma - \log\varepsilon_p$ graphs was very high (average value of $R^2 = 0.995$).

Fig. 9a shows that hydrogen has little or no effect on the strain-hardening behavior in either the transverse or normal orientations at room temperature.; in these cases n~0.05-0.06. However, when the deformation axis is aligned in the *rolling* direction, there is a significant increase in strain hardening with increasing hydrogen content. This effect is pronounced at room temperature (Fig. 9a) and persists to elevated temperatures; see Fig. 9b. Thus, while there is a consistent trend of decreasing strain hardening with increasing temperature (Fig. 9b), when deformed along the rolling direction, the material containing hydrides exhibits elevated strain hardening; in this case, a consistent increase of $\Delta n \approx 0.03$ occurs between room temperature and 300-400C.

The material property database, MATPRO [1], gives an expression for the strain-hardening exponent, n, as a function of temperature for Zircaloy-4 cladding tube (MATPRO does not currently contain an expression for n as a function of hydrogen content). The predicted n-value (based on data for tests along the cladding tube axis) as a function of temperature is plotted in Fig. 9b, and it lies significantly above (roughly a factor of two) the values measured in this study. On the other hand, the transverse stress-strain behavior of unhydrided Zircaloy-4 cladding tubes was determined by Link et al [3], and while the resulting n-values of n = 0.068 at 25°C and n = 0.059 at 300°C are close to the present n-values, they are also somewhat higher; see Fig.9b.

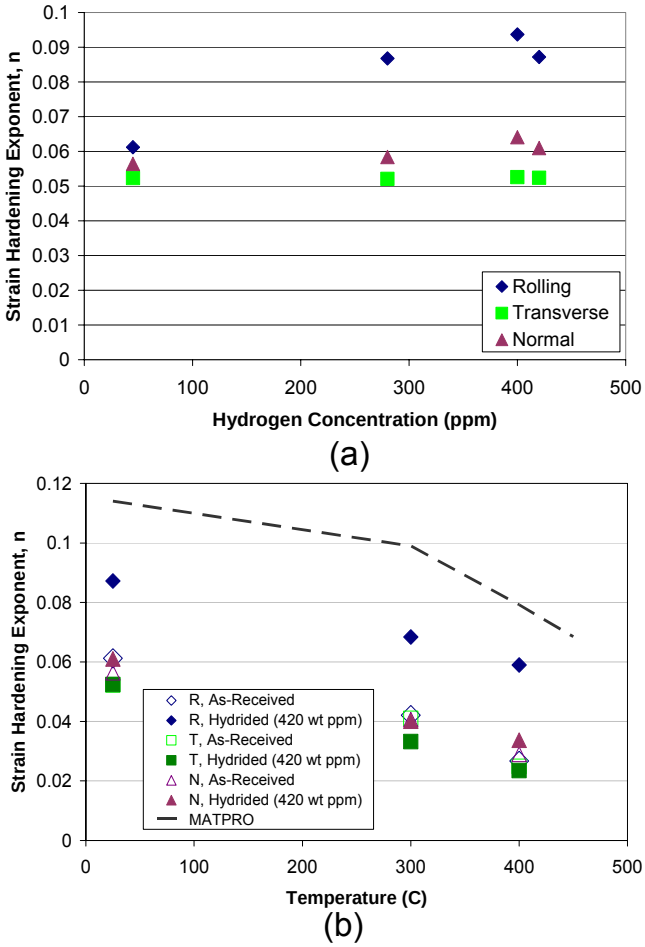

Figure 9. The strain-hardening exponent as a function of (a) hydrogen content at room temperature and (b) temperature for as-received and hydrided Zircaloy-4.

III.D. Strain Rate Hardening Behavior

The strain-rate hardening behavior was assessed assuming the material obeyed a rate dependence of the flow stress such that the strain-rate hardening exponent m could be defined as

$$m = d\ln\sigma / d\ln\dot{\varepsilon}_p \qquad (4)$$

where $\dot{\varepsilon}_p$ is the plastic strain rate. The m-value was determined experimentally from at least four measurements within a test during which the strain rate was changed instantaneously by factors of ten within the strain-rate range 10^{-4}/s to 10^{-1}/s. The resulting data shows that hydrogen has no significant effect on the m-value either at room temperature, Fig. 10a, or at elevated temperatures. Figure 10b shows that m ≈ 0.016 to 0.020 at both room temperature and 300°C, similar to values determined from previous observations [3]. However, at 400°C the strain-rate hardening exponent decreases in the rolling and transverse directions to m ≈ 0.012 to 0.013, and to m ≈ 0.014 in the normal orientation.

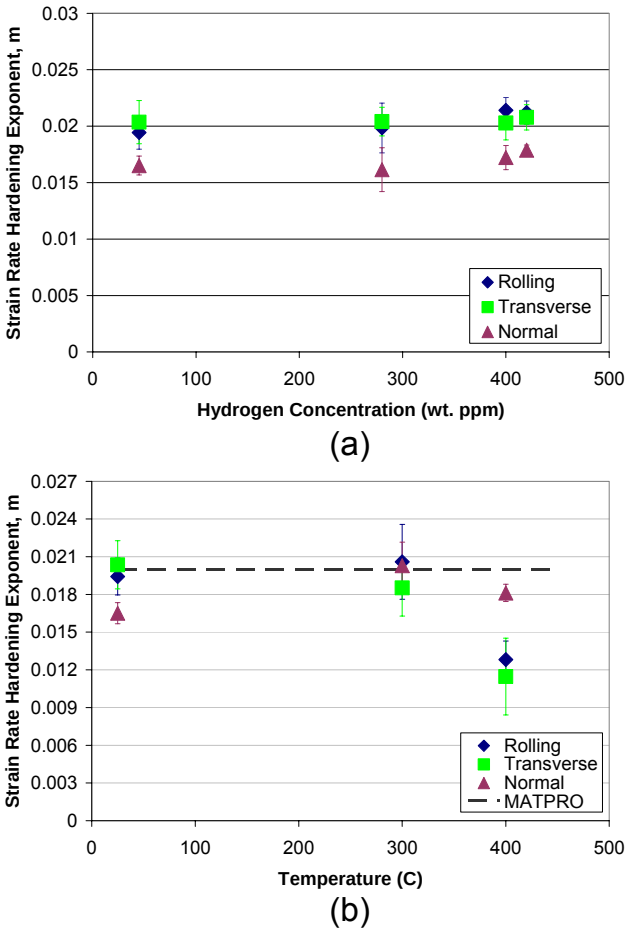

Figure 10. The strain-rate hardening exponent as a function of (a) hydrogen content at room temperature and (b) temperature for both hydrogen contents.

The material property database, MATPRO [1], also gives an expression for the strain-rate hardening exponent, m, as a function of temperature; MATPRO does not currently contain an expression for m as a function of hydrogen content. MATPRO reports a constant m-value below 457°C such that m = 0.02, as plotted in Fig. 10b. This study also obtains m = 0.02 at 25° and 300°C, but a small decrease in strain-rate hardening was observed at 400°C, earlier than that predicted by MATPRO; see Fig. 10b.

IV. CONCLUSIONS

The influence of hydrogen on the uniaxial deformation behavior of Zircaloy-4 was examined for plate material that was stress relieved after ~30% cold work following hot rolling. Compression testing of material containing ~45 wt ppm H to ~420 wt ppm H, over a range of temperatures (25°, 300°, and 400°C) and strain rates (10^{-4}/s to 10^{-1}/s) showed the following trends:

1. Increasing hydrogen content causes a small decrease in the 0.2% yield stress. This effect persists to elevated temperatures and is most pronounced for specimens oriented along the rolling direction.
2. For the three temperatures tested, the strain-hardening exponent is increased by hydrogen content when the stress axis is aligned with the rolling direction but not in the other two orientations.
3. The hydrogen content does not affect the strain-rate hardening exponent for any of the test temperatures or specimen orientations.
4. The plate material exhibits a strong degree of plastic anisotropy such that through-thickness deformation is quite difficult even at 400°C. As a result, the yield stress for specimens oriented with a compression axis aligned normal to the plate surface is roughly a factor of 1.8 higher than those oriented in either the rolling or transverse direction of the plate. This factor is close to that predicted using the Hill yield criterion and the experimentally determined plastic anisotropy parameters.
5. A plasticity analysis using the Hill yield criterion supports the notion that plastic deformation under through-thickness compression is equivalent to equal-biaxial tension at least for material exhibiting planar isotropy such as the present Zircaloy-4.
6. It was observed that the strain-hardening exponent in the rolling direction was influenced by hydrogen content, and therefore a material properties database such as MATPRO would benefit from an expression to quantify this effect for cladding tube material.

ACKNOWLEDGMENTS

We are very thankful for the financial support for this research program provided by the Nuclear Regulatory Commission under the supervision of Harold Scott, Ralph Meyer and John Voglewede. In addition, the authors acknowledge use of facilities at the Penn State University site of the National Science Foundation National Nanotechnology Infrastructure Network for the nickel coating vapor deposition. Finally, the expertise and experience of Patrick Raynaud was of great benefit during the experimental activities of this study.

REFERENCES

1. SCDAP/RELAP5/MOD3.3, Code Manual Vol. 4, Rev. 2: MATPRO: "A Library of Materials Properties for Light Water Reactor Accident Analysis", NUREG/CR-6150, INEL-96.0422, chapter 4.9., 2001.
2. S. Arsene, J. Bai, and P. Bompard, "Hydride embrittlement and irradiation effects on the hoop mechanical properties of pressurized water reactor (PWR) and boiling-water reactor (BWR) ZIRCALOY cladding tubes: Part III. Mechanical behavior of hydride in stress-relieved annealed and recrystallized ZIRCALOYs at 20C and 300C," *Metallurgical and Materials Transactions A: Physical Metallurgy and Materials Science*, **Vol. 34 A**, 3, 579-588, (2003).
3. T. M. Link, D. A. Koss, and A. T. Motta, "Failure of Zircaloy Cladding under transverse plane-strain deformation," *Nuclear Engineering and Design*, **vol. 186**, 379-394, (1998).
4. E. Tenckhoff, "Review of Deformation Mechanisms, Texture, and Anisotropy in Zirconium and Zircaloy", *Journal of ASTM International*, **vol. 2**, 25-50, (2005),.
5. P. Delobelle, P. Robinet, P. Bouffioux, P. Geyer, and I. Le Pichon, "A Unified Model to Describe the Anisotropic Viscoplastic Behavior of Zircaloy-4 Cladding Tubes", *ASTM STP 1295*, ASTM, Philadelphia, PA, pp. 373-393, 1996.
6. R. S. Daum, D. W. Bates, D. A. Koss, and A. T. Motta, "The influence of a hydrided layer on the fracture of Zircaloy-4 cladding tubes," *Proceedings of the International Conference on Hydrogen Effects on Material Behavior and Corrosion Deformation Interactions*, Sep 22-26, 2002, Moran, WY, United States, pp. 249-258 (2003).
7. A. Glendening, D. A. Koss, O. N. Pierron, A. T. Motta, and R. S. Daum, "Failure of Hydrided Zircaloy-4 Under Equal-Biaxial and Plane-Strain Tensile Deformation," *Journal of ASTM International*, **Vol. 2**, 6, paper ID12441, (2005).
8. O. N. Pierron, D. A. Koss, A. T. Motta, and K. S. Chan, "The Influence of Hydride Blisters on Fracture of Zircaloy 4," *Journal of Nuclear Materials*, **Vol. 322**, 21-35, (2003).
9. G. Bertolino, G. Meyer, and J. Perez Ipina, "Effects of hydrogen content and temperature on fracture toughness of Zircaloy-4," *Journal of Nuclear Materials*, **Vol. 320**, 3, 272-279, (2003).
10. P. H. Davies and C. P. Stearns, "Fracture Toughness testing of Zircaloy-2 Pressure Tube Material with Radial Hydrides Using Direct Current Potential Drop," *Fracture Mechanics: Seventeenth Volume, Seventeenth National Symposium on Fracture Mechanics.*, Albany, NY, USA, ASTM, Philadelphia, PA, USA, vol., 379-400, (1986).
11. S. B. Wisner and R. B. Adamson, "Combined Effects of Radiation Damage and Hydrides on the Ductility of Zircaloy-2," *GE Fuel*, **Vol. 3**, 1-21, (1996).
12. L. A. Simpson, "Criteria for Fracture Initiation at Hydrides in Zirconium-2.5% Niobium Alloy," *Metall. Trans.A*, **Vol. 12A**, 2113-2124, (1981).
13. M.L. Lovato and M.G. Stout, "Compression Testing Techniques to Determine the Stress/Strain Behavior of Metals Subject to Finite Deformation", *Metall. Trans. A*, **Vol. 23A**, 935-951, (1992).
14. R. O. Meyer, R. K. McCardell, H. M. Chung, D. J. Diamond, and H. H. Scott, "A Regulatory Assessment of Test data for Reactivity Initiated Accidents," *Nuclear Safety*, **Vol. 37**, 4, 872-387, (1996).
15. H. Stehle, E Steinberg, and E. Tenckoff, "Mechanical Properties, Anisotropy and Microstructure of Zircaloy Canning Tubes", ASTM STP 633, ASTM, Philadelphia, PA, pp. 486-507, 1977
16. J. J. Gilman and W. G. Johnston, "Movement of dislocations," *Metal Progress*, **Vol. 71**, 3, 76-77, (1957).
17. W.G. Johnston, "Yield Points and Delay Times in Single Crystals", *Journal of Applied Physics*, **Vol. 33**, 2716-2729, (1962).
18. R.W.K. Honeycombe, *The Plastic Deformation of Metals*, p150-156 Edward Arnold Publishers, London, 1968,
19. J. E. Bailey, "Electron microscope observations on the precipitation of Zirconium Hydride in Zirconium," *Acta Metallurgica*, **Vol. 11**, 267-280, (1963).
20. F. Pratt, M. Grange, J. Besson, and E. Andrieu, "Behavior and Rupture of Hydrided Zircaloy-4

Tubes and Sheets", *Metallurgical and Materials Transactions A*. **Vol. 29A** 1643-651, 1998
21. R. Hill, *The Mathematical Theory of Plasticity*, Clarendon Press, Oxford, 1950.
22. W.A. Backofen, *Deformation Processing*, Addison-Wesley Publishing, Cambridge, MA, 1972.